STUDYING THE EFFECT OF A TRIANGLE PROTRUSIONS DIMENSIONS ON HEAT TRANSFER AND FLUID FLOW OVER A HEATED FIN INSIDE RECTANGULAR DUCT

Dr. Ahmed Hashm Yousif
Mechanical Department
AL-Diwania Technical Institute

ABSTRACT:

A numerical study was carried out to investigate fluid flow and heat transfer over a heated fin (at constant heat flux) with using a triangle protrusions with Reynolds number range (350 – 2000) and Pr=0.71.

Different distance between the protrusions (b/H =0, 0.17, 0.33, 0.67, 1) with different height of protrusion (l/H =0.033, 0.067, 0.1) was used were (H) is the height of duct.

The geometrical configuration of interest is similar to a single element of a plate-fin cross flow heat exchanger. The installation of protrusion is organized, in such way that increased the surface of fin and mixed the flow near the fin with main flow.

A finite volume procedure was used to solve two dimensions conservation equations (mass, momentum and energy) with collocated grid. The results illustrate the essential significance of protrusion height and the distance between the protrusions base. Also, results show the heat transfer increasing with using protrusions as well as increasing pressure drop.

دراسة تأثير أبعاد النتؤات المثلثية على انتقال الحرارة والجريان على زعنفة ساخنة داخل مجرى مستطيل الشكل

الخلاصة

تم إجراء دراسة عددية لفحص الجريان وانتقال الحرارة على صفيحة مسخنة (زعنفة) بفيض حراري ثابت باستخدام النتؤات المثلثية لمدى من رقم رينولد(350-2000) ورقم براندتل 0.71 0

في هذه الدراسة تم فحص تأثير المسافات بين قواعد النتؤات (b/H =0, 0.17, 0.33, 0.67, 1) وتأثير ارتفاع النتؤات (l/H =0.033, 0.067, 0.1) على الجريان وانتقال الحرارة0

إن الترتيب الهندسي لهذه الدراسة هو شبيه بجزء من مبادل حراري متقاطع الجريان وان النتؤات التي وضعت قد أدت إلى زيادة مساحة الصفيحة وخلط المائع الساخن قرب السطح مع المائع الرئيسي البارد.

وقد تم استخدام طريقة الحجوم ألمحدده لحل المعادلات الحاكمة ثنائية البعد (الاستمرارية، الزخم والطاقة) مع استخدام الشبكة غير المتناوبة.

أظهرت النتائج إن للمسافة بين النتؤات وارتفاعها اثر كبير في الجريان وانتقال الحرارة حيث أن هذه النتؤات تزيد من انتقال الحرارة مع زيادة الهبوط بالضغط.

1- Introduction:

Compact heat exchangers are widely employed in engineering applications, especially in automotive, industry, air conditioning and refrigerant apparatus. The improvements in design of these heat exchangers have attracted many researchers for long time to develop more compact and less expansive heat exchanger with high energy performance [Ahmed et. al. (2003)].

In plate- fin or fin- tube heat exchangers the flow between the plates can be considered as a channel flow. For reduction the thermal resistance, the heat transfer coefficient need to be augmented [Tiggelbeek et. al.(1991)].

In plate–fin heat exchanger, the heat transfer coefficient is significantly low and in order to increase heat transfer between the fluid and plates, protrusions or vortex generators can be mounted [Biswas et. al. (1992)]. The influence of vortex generators and protrusions on fluid flow and heat transfer on flat plates was experimentally and numerically investigated. The researchers [Ahmed, et al. (2003)], [Biswas et. al.(1992)] and [Fiebig et. al. (1989)] are investigated flow and heat transfer on flat plate with using wing and winglet types vortex generators numerically, all of them found that the heat transfer enhanced by using vortex generators with increasing in pressure drop across the plates. The studies of [Tiggelbeek et. al.(1991)], [Isak et al.(1998)], [Mazen et. al. (1997)], [Yan et. al (2001)], [Russell et. al. (1982)] and [Edward et. al. (1974)] investigated the flow and heat transfer from plates with using obstacles and vortex generators experimentally. The studies shows that heat transfer enhanced with using obstacles and vortex generators therefore in present study a triangle prostrations will be used for enhanced heat transfer .

In present study the effect of the distance between protrusions (b) as well as the height of protrusions (l) will be investigated numerically as shown in fig. (1).

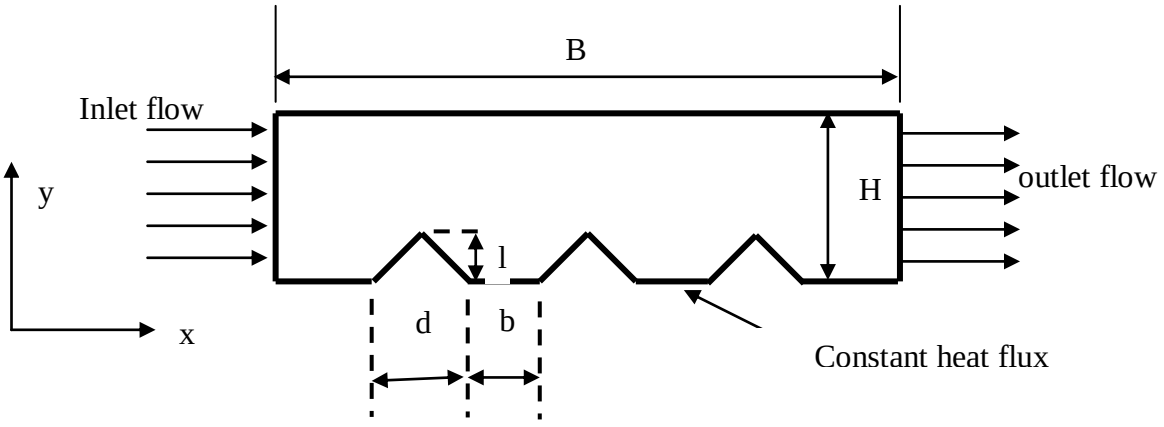

Figure (1) proposed flow domain

2- Mathematical model

The mathematical analysis is presented in a partial differential equation (PDE) which describe as

fully developing fluid flow.

Reynolds number at a range of Re=(350-2000)

parallel plate channel.
Incompressible flow.
steady state.

2-1 Grid Generation:

Figure (2) shows the schematic of two dimensions body fitting grid used for present computation. This grid was obtained by solving non homogeneous 2-D Laplace equations [Thompson et. al (1977)].

$$\xi_{xx}+ \xi_{yy} =P(\xi, \eta)$$

$$\eta_{xx}+ \eta_{yy}=Q(\xi, \eta) \qquad \text{……..1}$$

where P and Q are used to clustering the grid near the walls to sense the velocity gradient because there is a friction between the wall and the fluid. Equations (1) are transformed to (ξ, η) coordinates by interchanging the roles of dependent variables, this yield the following system equations.

$$\left.\begin{aligned} g_{11}x_{\xi\xi} - g_{21}x_{\xi\eta} + g_{22}x_{\eta\eta} &= -J^2(Px_{\xi}+Qx_{\eta}) \\ g_{11}y_{\xi\xi} - g_{21}y_{\xi\eta} + g_{22}y_{\eta\eta} &= -J^2(Py_{\xi}+Qy_{\eta}) \end{aligned}\right\} \qquad \text{----------2}$$

Where

$g_{11}= x_{\eta}^2 + y_{\eta}^2$

$g_{21}=2(x_{\xi}x_{\eta}+y_{\xi}y_{\eta})$

$g_{22}= x_{\xi}^2 + y_{\xi}^2$

$J=x_{\xi}y_{\eta}-x_{\eta}y_{\xi}$

Because the geometry of the domain was complex the (2-D) N-S, continuity and energy equations must be transported to general coordinates (ξ, η).

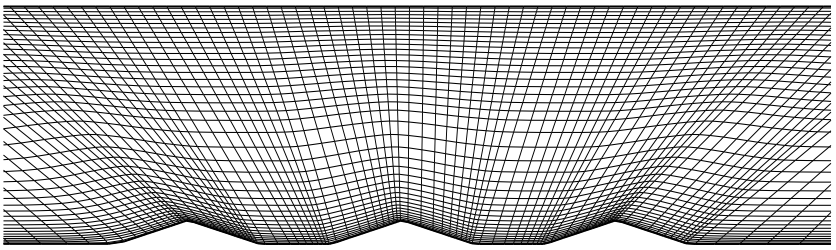

Figure (2) grid generated

2-2 Governing equations:

The 2-D governing equations of mass, momentum and energy equations for steady incompressible flow can be written as following:-

Continuity equation

$$\frac{\partial u}{\partial x}+\frac{\partial v}{\partial y}=0 \qquad \text{----------3}$$

Momentum equation

$$u\frac{\partial u}{\partial x}+v\frac{\partial u}{\partial y}=-\frac{1}{\rho}\frac{\partial p}{\partial x}+\nu\frac{\partial^2 u}{\partial y^2}$$

$$u\frac{\partial v}{\partial x}+v\frac{\partial v}{\partial y}=-\frac{1}{\rho}\frac{\partial p}{\partial y}+u\frac{\partial^2 v}{\partial x^2} \qquad \text{----------4}$$

Energy equation

$$u\frac{\partial T}{\partial x}+v\frac{\partial T}{\partial y}=\alpha\frac{\partial^2 T}{\partial y^2} \qquad \text{----------5}$$

The above equations can be written in a general transport equation as :-

$$\frac{\partial(\rho u\phi)}{\partial x}+\frac{\partial(\rho v\phi)}{\partial y}=\frac{\partial}{\partial x}\left[\Gamma_\phi(\frac{\partial\phi}{\partial x})\right]+\frac{\partial}{\partial y}\left[\Gamma_\phi(\frac{\partial\phi}{\partial y})\right]+S_\phi \qquad \text{----------6}$$

This equation serves as a starting point for computational procedure in (FVM) [Ferzingen et. al. (1999)]. The continuity equation can be obtained if (Φ=1, Γ_Φ=0 and S_Φ=0), by setting (Φ=u, v and Γ_Φ=μ, N-S equation can be obtain and energy equation can be obtained if (Φ=T and Γ_Φ=μ/pr). The two terms in the left of the general transport equation (Eq. 6) are convective terms, the first two terms in the right side of general transport equation (Eq. 6) are diffusive terms and the last term is the source term.

For the general curvilinear coordinates system (ξ, η), the general transport equation (Eq. 6) can be transformed to the following form:-

$$\frac{\partial}{\partial\xi}(\rho U\Phi-\frac{a1\Gamma_\Phi}{J}\frac{\partial\Phi}{\partial\xi})+\frac{\partial}{\partial\eta}(\rho V\Phi-\frac{a2\Gamma_\Phi}{J}\frac{\partial\Phi}{\partial\eta})=S_{NEW} \qquad \text{----------7}$$

where (U, V) are the contravariant velocity components (see figure (3)).

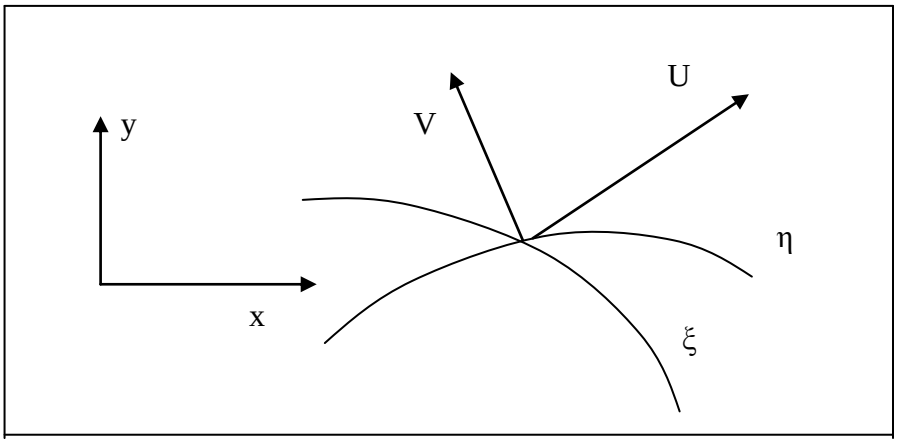

Figure (3) shows the contravariant velocity components

And $S_{NEW} = JS_{\Phi} + S_N$ where S_N is the source term due to non orthogonal characteristic of grid system which disappear under orthogonal grid system.

The transformation coefficients (a_1, a_2)are defined as:-

$$a_1 = \xi_x^2 + \xi_y^2$$
$$a_2 = \eta_x^2 + \eta_y^2$$
----------8

and the transformation metrics are calculated as follows

$$\left.\begin{aligned} \xi_x &= \frac{y_\xi}{J} \\ \xi_y &= \frac{-x_\eta}{J} \\ \eta_x &= \frac{-y_\xi}{J} \\ \eta_y &= \frac{x_\xi}{J} \end{aligned}\right\}$$
----------9

For collocated grid arrangement, all properties located at the center of control volume (P) as shown in fig. (4).

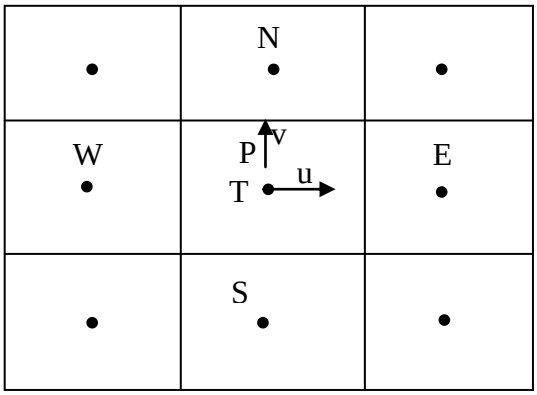

Figure (4) shows the control volumes

And the integration of equation (7) over control volume gives

$$[(\rho U\Phi)-(\frac{a1\Gamma_\Phi\Phi_\xi}{J})\Delta\eta]_w^e+[(\rho V\Phi)-(\frac{a2\Gamma_\Phi\Phi_\eta}{J})\Delta\xi]_s^n=dvS_{NEW} \quad \text{----------10}$$

where dv=Δξ Δη

To interpolate convection and diffusion terms, the power law difference scheme can be used Patenker (1980), and the following algebraic equation can be obtain:-

$$A_p\Phi_p = A_E\Phi_E+ A_W\Phi_W+ A_N\Phi_N+ A_S\Phi_S+ dv\ S_{NEW} \quad \text{----------11}$$

Where

$A_E=D_e*A(|P_{\Delta e}|)+[[-F_e, 0]]$
$A_W=D_w*A(|P_{\Delta w}|)+[[F_w, 0]]$
$A_N=D_n*A(|P_{\Delta n}|)+[[-F_n, 0]]$
$A_S=D_s*A(|P_{\Delta s}|)+[[F_s, 0]]$
$A_p= A_E+ A_W+ A_N+ A_S$

Where (F) is the mass flux and (D) is the diffusion term coefficient
In order to avoid the checkerboard pressure field in collocated grid system, a momentum interpolation technique on cell face was successfully proposed by Rhie and Chow interpolation method that developed by [Ferzigen et. al. (1999)].

2-3 Boundary conditions:

The (FVM)required that the boundary flux, either be known or expressed in term of known quantities on interior nodal value. the boundary of our solution include solid wall, inlet and outlet planes.

2-3-1 inlet boundary:

usually at inlet boundary, all quantities have to be prescribed as following:-
$(u)_{inlet}=u_{in}$, $(v)_{inlet}=v_{in}$, $(p)_{inlet}=p_{in}$, $(T)_{inlet}=T_{in}$

2-3-2 outlet boundary:

Always all values of dependent variables are unknown at exit boundary. It is often adequate to set outlet boundary values equal to intermediate up stream neighbor (e.g $\Phi_E=\Phi_p$). This is equivalent to saying the first derivative of property Φ in the direction normal to the boundary is equal to zero.

$$\frac{\partial u}{\partial x}=0,\frac{\partial v}{\partial x}=0,\frac{\partial p}{\partial x}=0 and\ \frac{\partial T}{\partial x}=0 \quad \text{----------12}$$

Wall boundary:

The velocity on the wall equal to zero
u=v=0 ----------13

The first derivative of pressure in the direction normal to the wall equal to zero

$$\frac{\partial p}{\partial y} = 0 \qquad \text{----------14}$$

For constant heat flux on bottom plane

$$T_w = q * \frac{y}{k} + T_{ij} \qquad \text{----------15}$$

and for adiabatic for top plate

$$\frac{\partial T}{\partial y} = 0 \qquad \text{----------16}$$

Heat transfer and pressure drop calculation:

The aim of present numerical study is to know logically the effect of distance between the protrusions and different height of protrusion on local heat transfer and pressure drop by calculation Nusselt number (Nu) and pressure coefficient (Cp) as follows.

2-4-1 Heat transfer calculation:

To calculate heat transfer (Nu) from heated wall at constant heat flux, first the temperature distribution can be calculated from the following equation.

$$q_{wall} = -k \frac{\partial T}{\partial n} \qquad \text{----------17}$$

where n is the normal distance
then calculate local Nusselt number (Nu_{ij})as following:-

$q_{wall}=q_{conv}$ ----------18

$q_{wall}=h_{(ij)}*(T_{(ij)}-T_b)$ ----------19

$Nu_{(ij)}=h_{(ij)}*H/k_f$ ----------20

2-4-2 Local static pressure coefficient

The Local static pressure coefficient along the wall surface can be calculated as following:-

$$cp_{(ij)}=\frac{(p_{(ij)} - p_o)}{0.5\rho u_{in}^2} \qquad \text{----------21}$$

3-Results and discussion

To investigate the flow and heat structure in plate-fin heat exchanger with protrusions at different position and different height, study of two dimensional simulations were carried out. In general, the main features of mean flow structure on flat plate can be shown in figure (5) and on plate with using protrusions at (b/H=0.33) with different heights (l/H=0.1, 0.067 and 0.033) at (Re=900) can be seen in figure (6- a, b, c).

The velocity distribution on a flat plate can be shown in figure (5) where the velocity gradient near the wall due to shear stress is clearly appeared. But when using protrusions as in figure (6 - a, b, c) the velocity distribution is clearly different, when the flow reaches the protrusions, the velocity will be increasing and change the direction toward the main flow and return toward the rear of protrusions faces due to low pressure and so on. Also, the figures show that protrusions height has an effect on velocity distribution and the small vortex will be appear when the protrusions be near together specially at high protrusions. Also, figure (7-a, b, c, d) shows the velocity distribution with using protrusions but with different Reynolds number. Where the velocity distribution is the same with different values

Figure (8) shows the temperature contour for flow in show duct without protrusions, where the temperature distributed from high temperature at the wall to the main flow temperature.

Temperature contours for a flow on plate with using protrusions can be shown in figure (9- a, b, c). The effect of protrusions on temperature distributions are clearly shown and the first protrusion is affect on the temperature distribution of the other protrusions and the duct surface specially at high protrusions.

Figure (10- a, b, c) show the effect of (b/H) ratio on pressure coefficient along the plate at Re = 900 and different (l/H) ratio and compared the results with free case. This figures shows that pressure will be dropping when using protrusions and the maximum peaks of pressure drop are tend to the center of plate when the ratio b/H tend to zero also, the curves show that the pressure coefficient have the same distribution with different values when using different protrusions heights.

Figure (11) show the comparison of pressure drop at different protrusion height with free case. As mentioned above, the pressure will be drop more when using protrusion due to increasing velocity near the protrusions and there is a different pressure across protrusion faces also pressure drop will be increasing when increases protrusion height.

Figure (12- a, b, c) show Nusselt number distribution along the plate with and without using protrusions. As it knows, heat transfer at flow without protrusions be high at the leading edge of the plate and decreasing toward the rear due to growth of boundary layer. In the case of flow with using protrusions the heat transfer will be increased when the flow reaches the front face of protrusion because the protrusions break up the boundary layer over the plate (fin) and increase the velocity. These lead to sweep the heat from the heated surface and lead to increasing heat transfer. Also, figures shows that when the ratio (b/H) tend to zero, the peaks of Nusselt number tend to the center of plate and local heat transfer continue in increasing because there is no enough distance to return the flow toward the rear faces of the protrusions.

Figure (13) show the comparison between Nusselt number distribution along the plate at Re=900 and b/H=0.33 with different heights of protrusions where heat transfer will be increasing with increasing heights of protrusions due to increasing the momentum of flow near the surface.

Figure (14) show the effect of Reynolds number on the average heat transfer from plate with using protrusions at b/H=0.33 and l/H=0.067, where the heat transfer increasing with the increases of Reynolds number due to increase the momentum of flow to sweep more heat from the surface of plate.

4-Conclusions

This study presents the numerical results for flow over plate with the existence of protrusions at different b/H and different l/H ratios at flow range from (Re=350 to 2000). The most important conclusions can be summarized at the follows:-

Heat transfer increased when using protrusions.

Heat transfer increased with the increasing of protrusions height.

There is an effect of the distance between the protrusions bases on local heat transfer and pressure drop.

Heat transfer increasing with increases Reynolds number.

Average heat transfer increased (15 % - 34 %) by using different protrusions height and different Reynolds number.

Average pressure drop increased (30 % - 50 %) by using different protrusions height and different Reynolds number.

5-References

Ahmed, S. and Lars, D. "Numerical study of heat and fluid flow in plate- fin heat exchanger with vortex generators " *Turbulence heat and mass transfer vol.4*, pp 1155-1162, 2003.

Tiggelbeek, S. Mitra, N. and Fiebig, M. "Comparison of wing type vortexgenerators for heat transfer enhancement in channel flows " *ASME*, vol. 116, pp 880-885, 1991.

Biswas, G. and Chattapdhyay, H "Heat transfer in channel with built - in wing type-vortex generators " *Int. J. heat mass transfer* vol.15, No.4, pp 803-814, 1992.

Fiebig, M. Brockmeier, U. Mitra, N. and Guntermann, T "Structure of velocityand temperature fields in laminar channel flow with longitudinal vortex generators" *Numerical heat transfer*, Part A, Vol.15, pp 281-302, 1989.

Isak, K. Teoman, A. Hayati, O. and Betiil, A. "Heat transfer and flow structure in rectangular channel with winglet type vortex generators " *Tr. J. of Engineering and Environmental Science*, vol.22, pp 185-195, 1998.

Mazen, M. O. and Robert, J. M. "An experimental investigation of the flow around a surface mounted pyramid" J. of Fluid Engineering vol. 115, pp 85-92, 1997.

Yan, W. M. Hsion, R. C. and Soony, C. Y. "experimental study of surface –mounted obstacle effects on heat transfer enhancement by using transient liquid crystal thermograph "*ASME*, 2001.

Russell, C. Jones, T. and Lee, G. "heat transfer enhancement using vortex generators " *Seventh int. heat transfer conf*. Munich, Federal Republic of Germany, pp 283-288, 1982.

Edward, F. J. and Alker, C. J. R. " The improvement of force convection heat transfer using surface protrusions in the form of (a)cubes and (b) vortex generators "Vth. Int. heat transfer conf., Tokyo, Japan 1974.

Ferzigen, J. and Peric, M. "*Computational method for fluid dynamic* " 2-th edition Springer, Berlin, 1999.

Yunliang, W. and Satoru, K. "Production of duct flows with a pressure- based procedure " *Numerical heat transfer*, Part A, vol.33, pp 723-748, 1998.

Thompson, J. F. Thomas, F. C. and Mastin "TOMACA-A code for numerical generation of boundary- fitted curvilinear coordinate system on field containing any number or arbitrary 2-D bodies " J. of computational physics, vol/24, pp 274- 303, 1977.

Patenker, S. V. "Numerical heat transfer and fluid flow.", Hemispere PublishingMc Graw- hill Book co., 1980.

Nomenclature

Symbol	Description	Unit
A	Convection-diffusion discritization coefficient	
a_1, a_2	Transformation coefficients	
B	Channel length	m
b	distance between the protrusions	m
Cp	Static pressure coefficient	
d	length of protrusion base	m
D	Diffusion term coefficient	
F	Mass flux	
H	Channel height	m
h_{ij}	Local heat transfer coefficient	$W/(m^2.K)$
J	Jacobean of transformation	
k	Thermal conductivity	W/(m. K)
l	Triangle protrusion height	m
n	Normal distance	
Nu	Nusselt number	
P	Source term in grid generation system of equation	
P_0	Total pressure	N/m^2
P_{ij}	Local static pressure	N/m^2
Pr	Prandtl number	
q	Heat flux per unit area	W/m^2
Q	Source term in grid generation system of equation	

S	Source term for the dependent variable Φ	
T	Temperature	K
u	Velocity in x-direction	m/s
U, V	Contravariant velocities	
v	Velocity in y- direction	m/s
x, y	Cartesian coordinates	

Greek Symbols

Symbol	Description	Unit
ξ, η	General coordinates	
Φ	General variable	
ρ	Density	Kg/m^3
Γ	Coefficient of Diffusivity	

Abbreviation

Symbol	Description	Unit
2-D	Two dimensions	
FVM	Finite volume method	
N-S	Naveir-Stoke equation	
PDE	partial differential equation	

Subscripts

Symbol	Description	Unit
b	Bulk	
e, w, n, s	Faces of control volume	
E, W, N, S	Neighbor nodes of node P	
f	fluid	
P	Center of control volume	
ij	Index counter in (x, y) or (ξ, η) directions	
in	Inlet condition	
Φ	Total source of Φ transport property	
w	Wall	

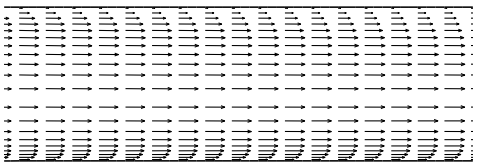

Figure (5) velocity distribution
Without protrusions , Re=900

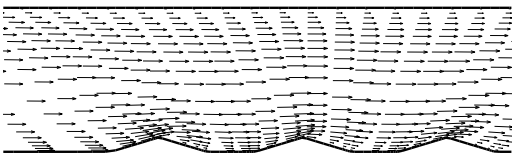

Figure (6-a) velocity distribution with
protrusions at b/H=0.33, l/H=0.1, Re=900

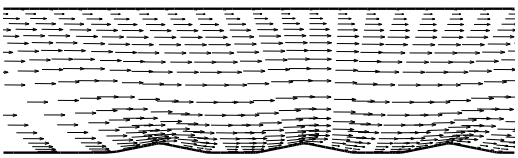

Figure (6-b) velocity distribution with
protrusions b/H=0.33, l/H=0.067,Re=900

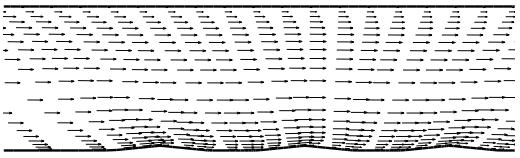

Figure (6-c) velocity distribution at with
protrusions at b/H=0.33, l/H=0.033, Re=900

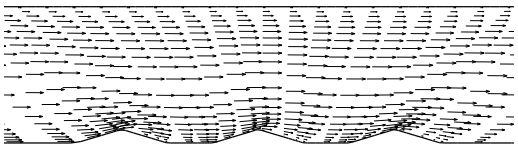

Figure (7-a) velocity distribution with
protrusions at b/H=0.33, l/H=0.1,Re=900

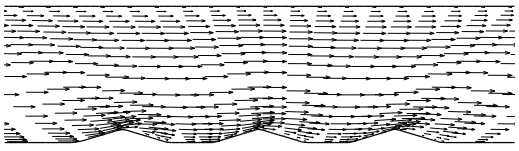

Figure (7-b) velocity distribution at with
protrusions at b/H=0.33, l/H=0.1, Re=2000

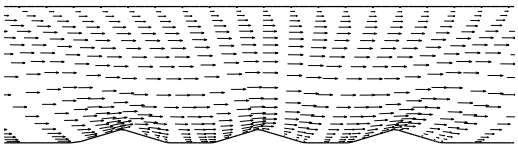

Figure (7-c) velocity distribution with protrusions at b/H=0.33, l/H=0.1,Re=750

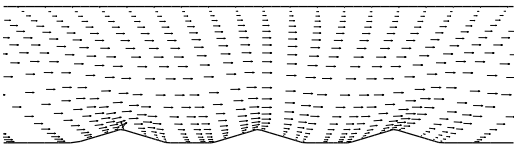

Figure (7-d) velocity distribution at with protrusions at b/H=0.33, l/H=0.1, Re=350

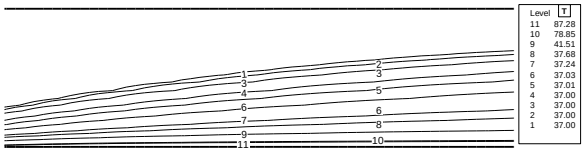

Figure (8) Temperature contour Without protrusions. Re=900

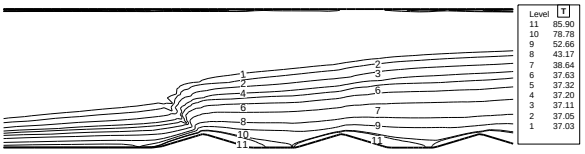

Figure (9-a) Temperature contour with protrusions at b/H=0.33, l/H=0.1, Re=900

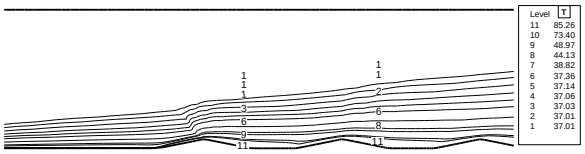

Figure (9-b) Temperature contour with protrusions b/H=0.33, l/H=0.067, Re=900

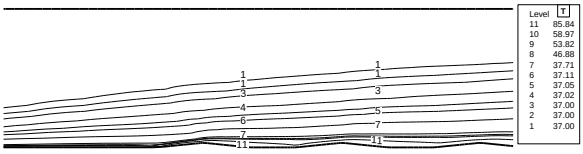

Figure (9-c) Temperature contour with protrusions at b/H=0.33, l/H=0.033, Re=900

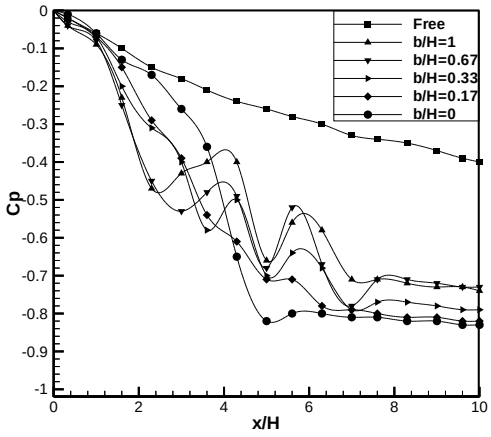

Figure (10-a) pressure coefficient along the plate at l/H=0.1, Re=900

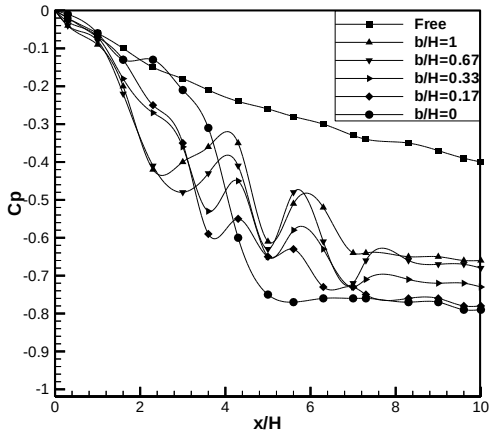

Figure (10-b) pressure coefficient along the plate at l/H=0.067, Re=900

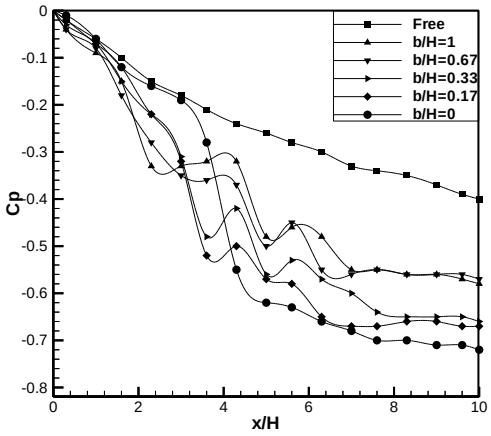

Figure (10-c) pressure coefficient at b/H=0.33

Re=900with different l/H

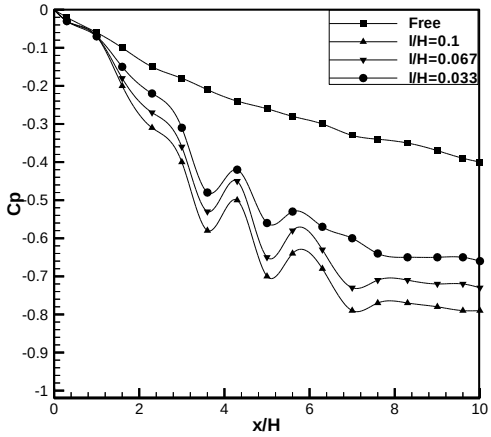

Figure (11) pressure coefficient at b/H=0.33

Re=900with different l/H

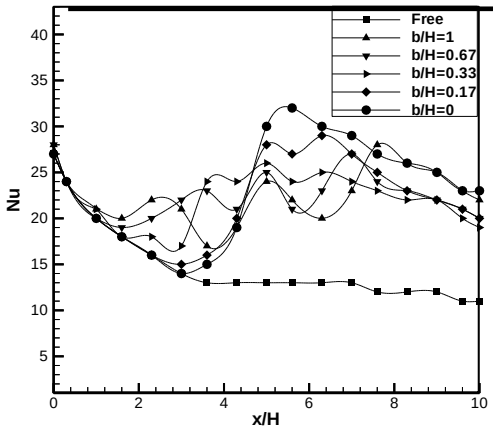

Figure (12- a)Nusselt number distribution at l/H=0.1, Re=900

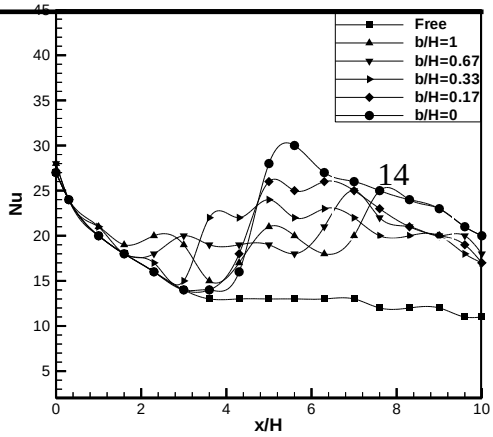

Figure (12- b)Nusselt number distribution at l/H=0.067, Re=900

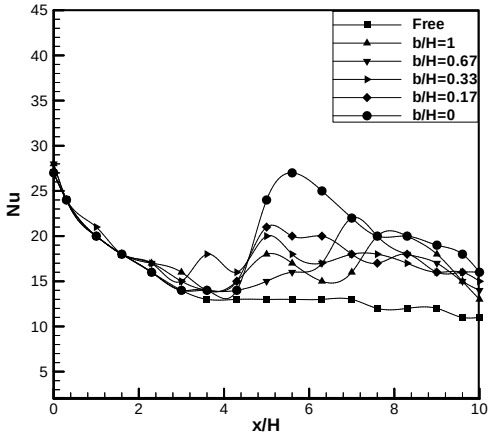

Figure (12- c)Nusselt number distribution at l/H=0.033, Re=900

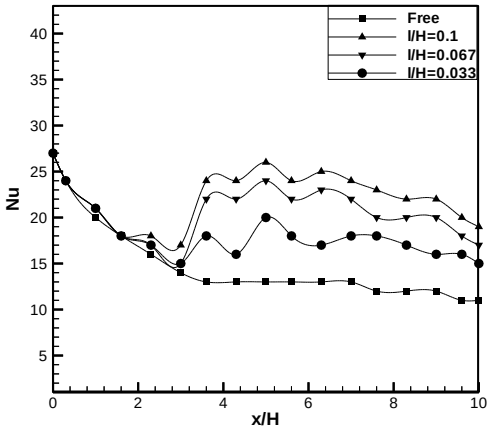

Figure (13)Nusselt number distribution at b/H=0.33, Re=900 with deferent l/H

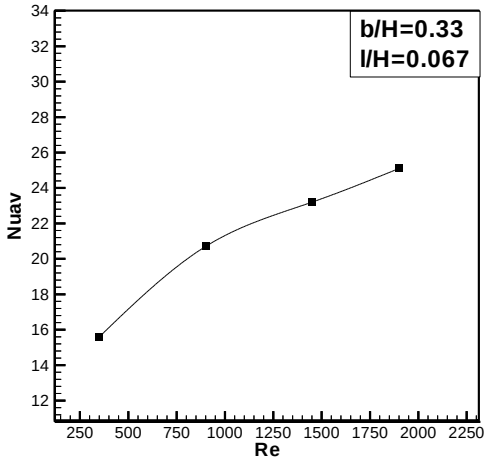

Figure (14) effect of Reynolds number on Nusselt number